Available online at www.sciencedirect.com

SCIENCE DIRECT

Brain Research 1027 (2004) 48–58

BRAIN RESEARCH

www.elsevier.com/locate/brainres

Research report

Nicotine increases in vivo blood–brain barrier permeability and alters cerebral microvascular tight junction protein distribution

Brian T. Hawkins[a], Thomas J. Abbruscato[b], Richard D. Egleton[c], Rachel C. Brown[d], Jason D. Huber[e], Christopher R. Campos[c], Thomas P. Davis[a,c,*]

[a]Program in Neuroscience, College of Medicine, The University of Arizona, Tucson, AZ 85724, United States
[b]Department of Pharmaceutical Sciences, School of Pharmacy, Texas Tech University Health Sciences Center, Amarillo, TX 79106, United States
[c]Department of Pharmacology, College of Medicine, The University of Arizona, Tucson, AZ 85724, United States
[d]Department of Integrative Biology and Pharmacology, University of Texas Health Science Center, Houston, TX, 77030, United States
[e]Department of Basic Pharmaceutical Sciences, West Virginia University, Morgantown, WV 26506, United States

Accepted 19 August 2004
Available online 18 September 2004

Abstract

The blood–brain barrier (BBB) is critical to the health of the central nervous system. The BBB is formed primarily by the presence of tight junctions (TJ) between cerebral microvessel endothelial cells. In light of the known effects of nicotine on endothelial cell biology, the specific effects of nicotine on the in vivo BBB were examined. Using in situ brain perfusion, it was found that continuous administration of nicotine (4.5 mg free base $\cdot kg^{-1} \cdot day^{-1}$) for 1 and 7 days led to increased permeability of the BBB to [^{14}C]-sucrose without significant changes in its initial volume of distribution. The expression and distribution of the TJ-associated proteins actin, occludin, claudin-1, -3, and -5, and ZO-1 and -2 were analyzed by Western blot and immunofluorescence microscopy. Though no changes in total protein expression were observed, nicotine treatment was associated with altered cellular distribution of ZO-1 and diminished junctional immunoreactivity of claudin-3. It is proposed that nicotine leads to changes in BBB permeability via the modulation of TJ proteins.

Theme: Cellular and molecular biology
Topic: Blood–brain barrier

Keywords: Blood–brain barrier; Nicotine; Tight junction; ZO-1; ZO-2; Claudin

1. Introduction

The blood–brain barrier (BBB) is a vascular system that regulates the passage of materials between the peripheral circulation and the central nervous system (CNS). The BBB is essential for maintaining brain homeostasis and enabling proper neuronal function [32,53] but makes the non-invasive delivery of therapeutics to the brain problematic [48]. Situated at the level of the cerebral microvascular endothelium [44], the BBB presents a diffusion barrier to most non-lipophillic molecules [33]. The barrier is established by a lack of fenestrations [13] and the presence of tight junctions (TJ) in the apical region of the interendothelial cleft. TJ are elaborate, interconnected membrane-spanning structures composed of transmembrane proteins linked via accessory proteins to the actin cytoskeleton [59] found in epithelial and endothelial barrier tissues throughout the body. Once thought to be static structures, TJ are in fact regulated in both physiological and pathological states [25], and changes in TJ protein expression and/or organization have been associated with altered permeability [4,15,27,37,46,62].

* Corresponding author. 1501 North Campbell Avenue, P.O. Box 245050, Tucson, AZ, 85724-5050, United States. Tel.: +1 520 626 7643; fax: +1 520 626 4053.
E-mail address: davistp@u.arizona.edu (T.P. Davis).

0006-8993/$ - see front matter © 2004 Elsevier B.V. All rights reserved.
doi:10.1016/j.brainres.2004.08.043

Approximately 23% of people in the United States smoke cigarettes [5]. Cigarette smoking is associated with increased risk of cancer, lung disease, and cardiovascular disease including cerebrovascular disease [19]. Though cigarette smoke contains more than 4000 chemical constituents [22], the alkaloid nicotine merits special consideration with regard to vascular disease. In addition to being the primary mediator of the subjective and potentially addictive effects of tobacco [42], nicotine has profound effects on vascular tissues including stimulation of abnormal DNA synthesis in endothelial cells [58], increased expression of atherogenic genes [65], altered expression of signal transduction and transcription factor genes [66], and angiogenesis [20,21].

The effect of nicotine on the BBB is controversial. One study found that acute nicotine at non-toxic concentrations had no effect on the permeability of large molecular weight markers at the BBB [49], though this finding did not rule out the possibility that nicotine may disrupt the BBB to passage of smaller molecules [31]. In subsequent chronic studies, non-toxic doses of nicotine altered both the expression and function of ion [2,60] and glucose transporters [9,10] in cerebral microvessels. Additionally, we have reported that nicotine and its major metabolite cotinine increase the permeability of an in vitro model of the BBB, and that this change is associated with diminished expression and altered distribution of the TJ protein ZO-1 mediated by endothelial nicotinic acetylcholine receptors [1].

In the current study, nicotine was infused via subcutaneous osmotic pumps into Sprague–Dawley rats in a dosing regimen designed to sustain plasma nicotine and cotinine concentrations comparable to those found in human smokers. Using modifications of the in situ brain perfusion method of Takasato [55], we investigated the effects of nicotine on in vivo BBB permeability. Expression and distribution of the TJ-associated proteins ZO-1, ZO-2, occludin, claudin-1, -3, and -5, and the cytoskeletal protein actin were examined using Western blot analysis and fluorescent immunohistochemistry.

2. Materials and methods

2.1. Radioisotopes, antibodies, and chemicals

[^{14}C]-Sucrose was purchased from ICN Pharmaceuticals (specific activity, 462 $mCi \cdot mol^{-1}$; Irvine, CA). Mouse monoclonal anti-actin was purchased from Sigma (St. Louis, MO). Rabbit polyclonal anti-ZO-1 and -2, rabbit polyclonal anti-claudin-1 and -3, mouse monoclonal anti-claudin-5 and anti-occludin were purchased from Zymed (San Francisco, CA). Conjugated anti-mouse and anti-rabbit IgG-horseradish peroxidase were obtained from Amersham (Springfield, IL). Alexafluor™ 488-conjugated phalloidin and Alexafluor™ 488-conjugated anti-rabbit and anti-mouse IgG were obtained from Molecular Probes (Eugene, OR). All other reagents, unless otherwise stated, were purchased from Sigma.

2.2. Animals and treatments

All animal protocols used in this study were approved by the University of Arizona Institutional Animal Care and Use Committee and conform to National Institutes of Health (NIH) guidelines. Female Sprague–Dawley rats (Harlan Sprague–Dawley, Indianapolis, IN) weighing 240–300 g were housed under standard 12:12-h light/dark conditions and received food and water ad libitum. Animals were implanted with Alzet 2ML4 osmotic pumps (Alza, Palo Alto, CA) for continuous subcutaneous delivery of nicotine at 4.5 mg free base $\cdot kg^{-1} \cdot day^{-1}$ (nicotine hydrogen tartrate dissolved in 0.9% saline) or 0.9% saline alone as a time-matched control. Animals were anesthetized with 1 $ml \cdot kg^{-1}$ of a cocktail containing ketamine (78.3 $mg \cdot ml^{-1}$), acepromazine (0.6 $mg \cdot ml^{-1}$), and xylazine (3.1 $mg \cdot ml^{-1}$). A 1-cm transverse incision was made between the scapula, and the pump was inserted under the skin posterior to the incision, which was closed with wound clips. The animals were treated with gentamycin (0.1 $mg \cdot kg^{-1}$) to prevent infection, and allowed to recover in individual cages for the duration of their treatment. At 1 or 7 days post-implantation, animals underwent in situ brain perfusion or the brain was harvested for cerebral microvessel isolation.

2.3. HPLC analysis of plasma nicotine and cotinine

Whole blood was extracted from the tail vein prior to sacrifice. Nicotine and cotinine were extracted from rat plasma and HPLC analysis performed based on the methods of Dawson [8]. Plasma (500 μl) was added to a 1.5-ml centrifuge tube containing 10 μl 2-phenylimidizole (15 $ng \cdot \mu l^{-1}$), 20 μl 5% antifoam/phenol red solution, 50 μl 30% NH_4OH, and 500 μl dichloroethane and mixed by gentle inversion for 1 min. The solution was centrifuged 15 min using a Beckman Microfuge 11 (12,000 rpm). The supernatant was discarded and 400 μl of the clear bottom layer was placed into a 1.5-ml tube and dried under N_2. HPLC buffer (300 μl; 30 mM citric acid, 30 mM KH_2PO_4, 3.65 $g \cdot L^{-1}$ triethylamine, 0.6 $g \cdot L^{-1}$ 1-heptanesulfonic acid, 90 $ml \cdot L^{-1}$ acetonitrile, pH 4.8) was added to the tube. A standard curve was generated using rat plasma extractions of 0, 12.5, 25, 50, 100, and 200 $ng \cdot ml^{-1}$ of nicotine and cotinine and 150 ng of 2-phenylimidizole added as an internal standard.

HPLC analysis of plasma nicotine and cotinine was performed on a 0.46×15 cm Inertsil™ ODS-2 column (MetaChem Technologies, Torrance, CA) at a flow rate of 1.0 $ml \cdot min^{-1}$ at 37°C for 7.5 min and then increased to 1.5 $ml \cdot min^{-1}$ for 8 min. All samples were injected using a Waters Associates WISP™ 712B autoinjector. Separations were achieved using an isocratic mobile phase (HPLC buffer). Nicotine, cotinine, and 2-phenylimidizole were detected by a Shimadzu SDP-6A UV spectrophotometric

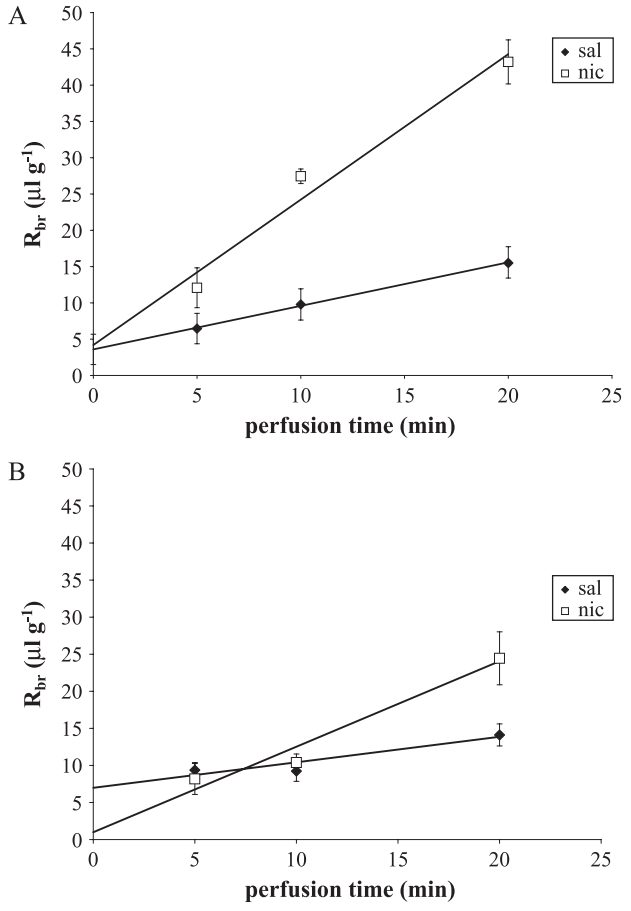

Fig. 1. In situ brain perfusion with [^{14}C]-sucrose: (A) 1-day treatment; (B) 7-day treatment. R_{br} are means±S.E.M., n=5–11 per time point. Nicotine significantly increases the rate of [^{14}C]-sucrose uptake into the brain (K_{in}), without a significant change in vascular volume (V_D). Significance was determined by comparison of the regression coefficients as described by Glantz [16].

detector (254 nm) and peaks were integrated with a Hewlett Packard 3396A integrator.

2.4. In situ brain perfusion

Animals were anesthetized as above and heparinized by i.p. injection (10,000 U·kg^{-1}). A ventral midline incision was made at the neck, and the common carotid arteries were exposed. The arteries were cannulated with silicone tubing and the jugular veins were cut. The perfusion medium consisted of a mammalian Ringer's solution (117 mM NaCl, 4.7 mM KCl, 0.8 mM $MgSO_4$, 24.8 mM $NaHCO_3$, 1.2 mM KH_2PO_4, 2.5 mM $CaCl_2$, 10 mM D-glucose, 39 g·L^{-1} dextran (MW 70 kDa), 10 g·L^{-1} BSA, pH 7.4) containing Evans blue-labeled albumin. The medium was oxygenated with 95% O_2 and 5% CO_2. The perfusate was passed via peristaltic pump through a heating coil (37°C) and a bubble trap. Once the desired perfusion pressure and rate were achieved (approximately 100 mm Hg and 3.1 ml·min^{-1}), [^{14}C]-sucrose (10 μCi per 20 ml Ringer) was infused (0.5 ml·min^{-1} per hemisphere) using a slow-drive syringe pump (model 22; Harvard Apparatus, South Natick, MA). The animal was perfused for 5–20 min, after which the animal was decapitated and the brain removed. Samples of the radioactive perfusate were collected from each carotid cannula as a reference. The choroid plexuses were excised and the meninges removed, and the cerebral hemispheres were sectioned and homogenized. Brain tissue and 100-μl samples of perfusate were prepared for liquid scintillation counting by incubation in 1-ml tissue solubilizer (TS-2, Research Products, Mount Pleasant, IL) for 2 days. Prior to counting, 100 μl 30% acetic acid and 4 ml Budget-Solve Liquid Scintillation Cocktail (Research Products) were added, and the samples were measured for radioactivity (model LS 5000 TD Counter; Beckman Instruments, Fullerton, CA). Results are reported as the ratio of radioactivity in the brain to that in the perfusate (R_{br}):

$$R_{br}(\mu l\ g^{-1}) = \left(C_{brain}(\text{dpm}\ g^{-1})/C_{perfusate}(\text{dpm}\ \mu l^{-1})\right). \quad (1)$$

A least-squares regression of R_{br} vs. perfusion time was performed for each experimental and control group:

$$R_{br}(T) = V_D + K_{in}T \quad (2)$$

where V_D is the initial volume of distribution of [^{14}C]-sucrose, K_{in} is the unidirectional transfer coefficient, and T is the perfusion time in minutes.

2.5. Cerebral microvessel isolation

Animals were anesthetized as described above and decapitated. The brain was removed from the skull, the meninges and choroid plexuses were removed, and the brainstem and cerebellum were dissected away from the cerebral hemispheres. The hemispheres were homogenized in a fivefold volume of buffer (103 mM NaCl, 4.7 mM KCl, 2.5 mM $CaCl_2$, 1.2 mM KH_2PO_4, 1.2 mM $MgSO_4$, 15 mM HEPES, 25 mM $NaHCO_3$, 10 mM glucose, 1 mM sodium pyruvate, 10 g·L^{-1} 64 K dextran), suspended in an equal volume of 26% dextran, and centrifuged for 10 min at 5800×g at 4 °C. The pellet was resuspended and passed through a 100-μm mesh. The filtrate was centrifuged for 10 min at 1500 rpm at 4 °C, and the resulting pellet was resuspended in 0.25 ml buffer.

Table 1
Analysis of multiple-time uptake regression coefficients

	1-day		7-day	
	Saline	Nicotine	Saline	Nicotine
K_{in} (μl·g^{-1}·min^{-1})	0.6±0.2	2.0±0.3[a]	0.3±0.1	1.2±0.3[b,c]
V_D (μl·g^{-1})	3.6±2.5	4.2±3.6	7.0±1.7	1.0±4.2

Data are the regression coefficients of the plots shown in Fig. 1 ±S.E. Significance was determined by the methods for comparing linear regressions described by Glantz [16].

[a] p<0.01 vs. time-matched saline control.

[b] p<0.05 vs. time-matched saline control.

[c] p<0.05 vs. 1-day nicotine.

2.6. Western blot

Protein was extracted from brain microvessels by incubating overnight in 6 M urea buffer (6 M urea, 10 mM Tris, 1 mM dithiothreitol, 5 mM $MgCl_2$, 5 mM EGTA, 150 mM NaCl, pH 8.0, 1 tablet Complete mini EDTA-free protease inhibitor per 10 ml (Roche, Mannheim, Germany)) at 4 °C. Protein was quantified using the bicinchoninic acid method (Pierce, Indianapolis, IN) with BSA as a standard.

Protein samples (50 μg) were separated using an electrophoretic field on Novex 4–12% Tris–glycine gels (Invitrogen, Carlsbad, CA) at 100 V for 120 min. Proteins were transferred to polyvinylidene fluoride membranes with 240 mAmp at 4 °C for 45 min. The membranes were blocked using 5% non-fat milk/Tris-buffered saline (TBS) (20 mM Tris base, 137 mM NaCl, pH 7.6) with 0.1% Tween-20. Following blocking, membranes were incubated with primary antibody (anti-actin, 1:1000, anti-occludin, 1:500, anti-ZO-1, 1:1000, anti-ZO-2, 1:1000, anti-claudin-1, 1:1000, anti-claudin-3, 1:500, or anti-claudin-5, 1:1000) 1 h at RT. Membranes were washed with 5% non-fat milk/TBS buffer prior to incubation with the appropriate secondary

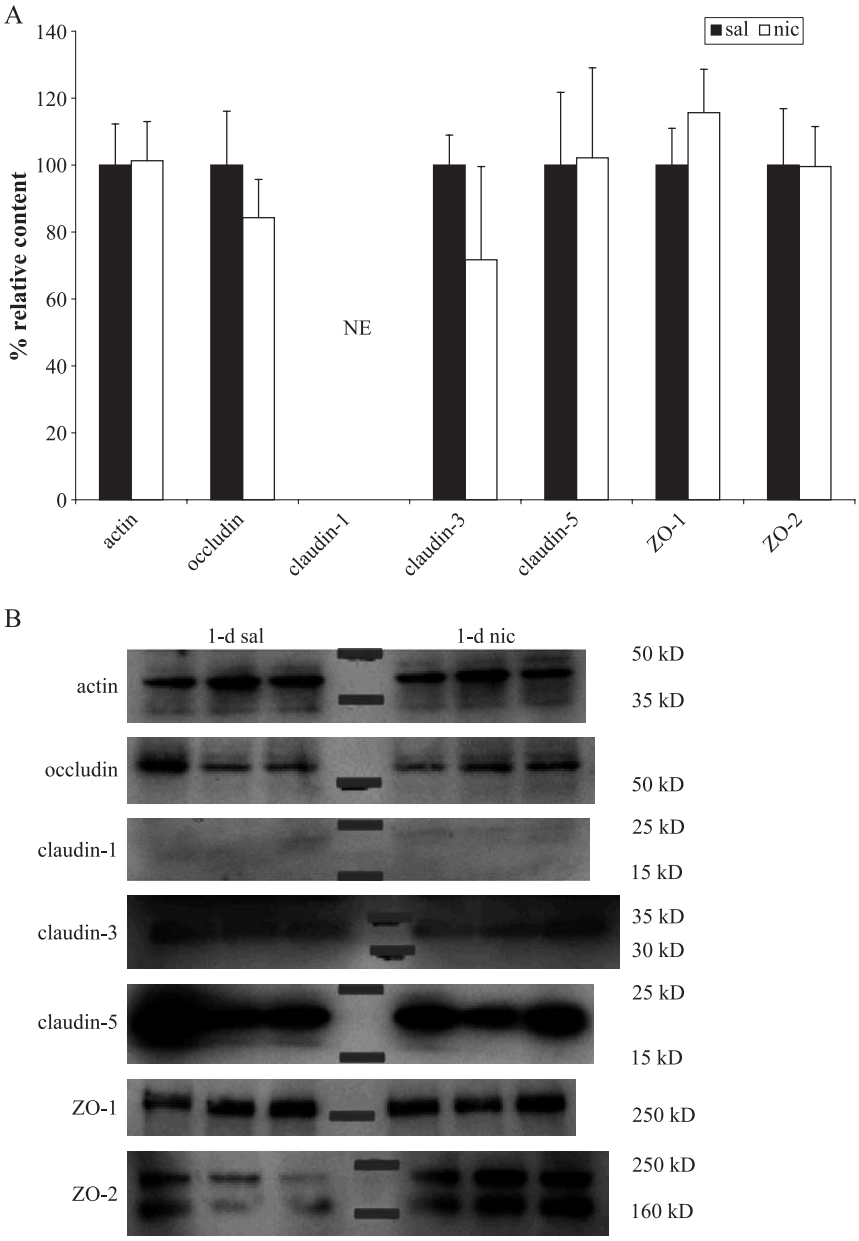

Fig. 2. Western blot analysis of TJ proteins in brain microvessels. (A) Summary of 1-day treatment; (B) representative blots from 1-day treatment; (C) summary of 7-day treatment; (D) representative blots from 7-day treatment. Total protein was extracted from rat brain microvessels. Band densities were normalized to the mean density of saline bands and expressed as % relative content. Gel staining was used as a loading control. Bars are mean % relative content±S.E.M., n=6 for each group. Significance was determined by Student's t test, nicotine vs. time-matched control; p>0.05 for all comparisons. NE=not expressed.

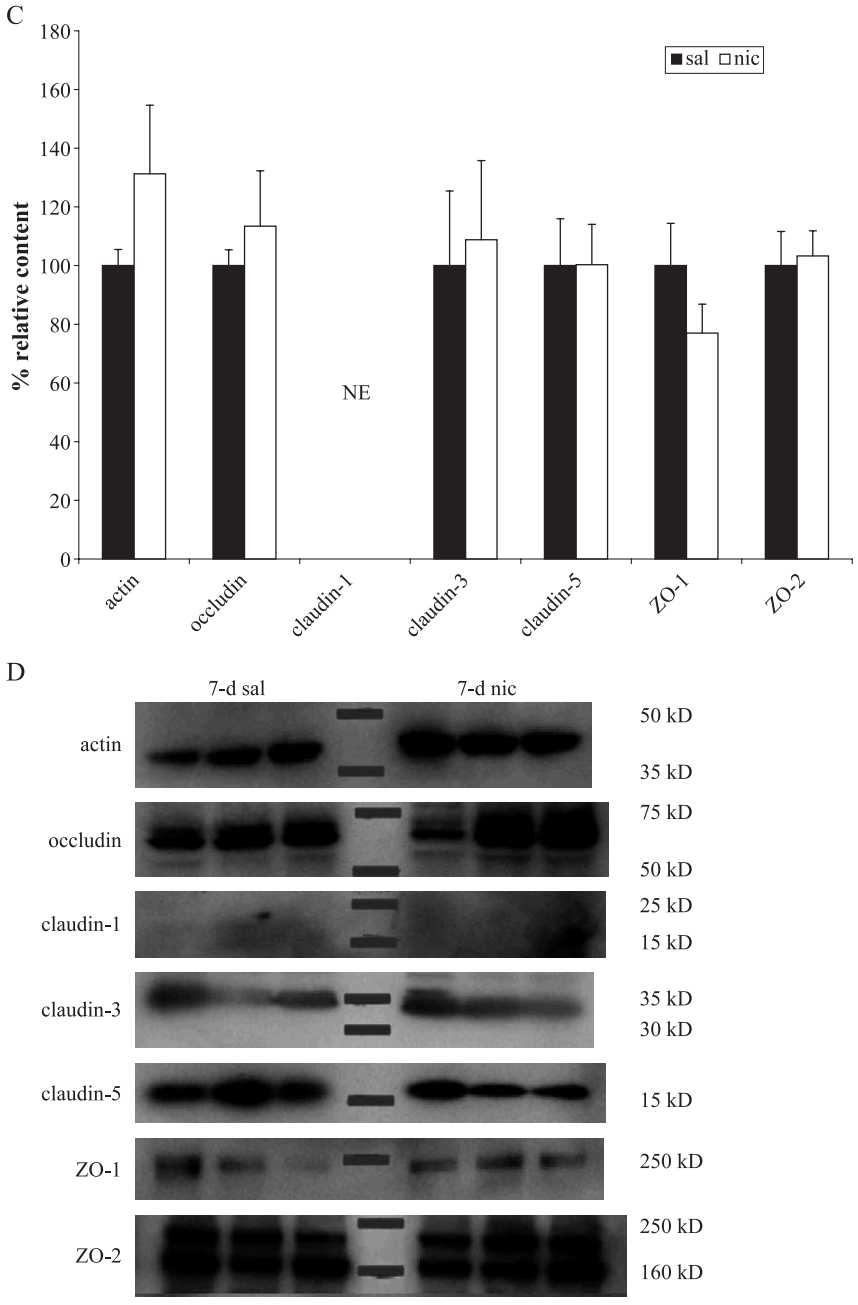

Fig. 2 (*continued*).

antibody (anti-mouse, 1:3000 or anti-rabbit, 1:2000) for 30 min at room temperature. Membranes were developed using the enzyme chemiluminescence method (ECL^{plus}; Amersham) and protein bands were visualized on X-ray film. Semi-quantitation of protein was performed with a Kodak Image Station. Gel staining (Gelcode; Pierce, Rockford, IL) was used as a loading control. Results are reported as percent expression of control.

2.7. Immunofluorescence microscopy

Microvessels isolated as described above were smeared onto microscope slides and heat-fixed at 95 °C, 10 min. The vessels were fixed with 3.7% formaldehyde in PBS, permeabalized with 0.1% Triton X-100 in PBS, and blocked for 1 h in 1% BSA in PBS. To visualize actin, slides were incubated with Alexafluor™ 488-conjugated phalloidin (reconstituted in 1% BSA in PBS, 5 U · ml^{-1}) for 30 min. To visualize the other proteins, slides were incubated with primary antibody (mouse anti-occludin, 1:100, mouse anti-claudin-1, 1:100, rabbit anti-claudin-3, 1:200, mouse anti-claudin-5, 1:100, rabbit anti-ZO-1, 1:200, or rabbit anti-ZO-2, 1:100) diluted in 1% BSA in PBS for 30 min, rinsed with 1% BSA in PBS, and incubated with Alexafluor™ 488-conjugated anti-rabbit or anti-mouse IgG (2 μg · ml^{-1}) for 30 min. Vessels from nicotine-treated animals were always

stained alongside vessels from a time-matched control for the same protein. After placement and sealing of coverslips, photographs were taken with 100× oil immersion objectives on a Nikon TE300 fluorescent microscope with a fluorescein filter.

The distribution of tight junction proteins in isolated cerebral microvessels was assessed according to the method of Song [52] using Metamorph™. Briefly, the mean pixel intensity was measured within ten 49-pixel (7×7) areas selected at random along the margins of cell–cell contact when visible, or along the length of a vessel when the cellular margins were not clearly stained. Measured mean pixel intensities were normalized to background levels within each image. Measurements were taken by an investigator blinded to both the target protein and treatment group. Results are reported as percentage of control.

2.8. Data analysis

For in situ brain perfusion experiments, statistical comparisons of the regression coefficients K_{in} and V_D were performed according to the methods of Glantz [16]. Analysis of all other data was performed by Student's t test for comparison of two means (nicotine vs. time-matched control).

3. Results

3.1. HPLC analysis of plasma nicotine and cotinine

To confirm the osmotic pump delivery of nicotine, plasma levels of nicotine and cotinine were measured by HPLC in blood samples collected from the tail vein prior to

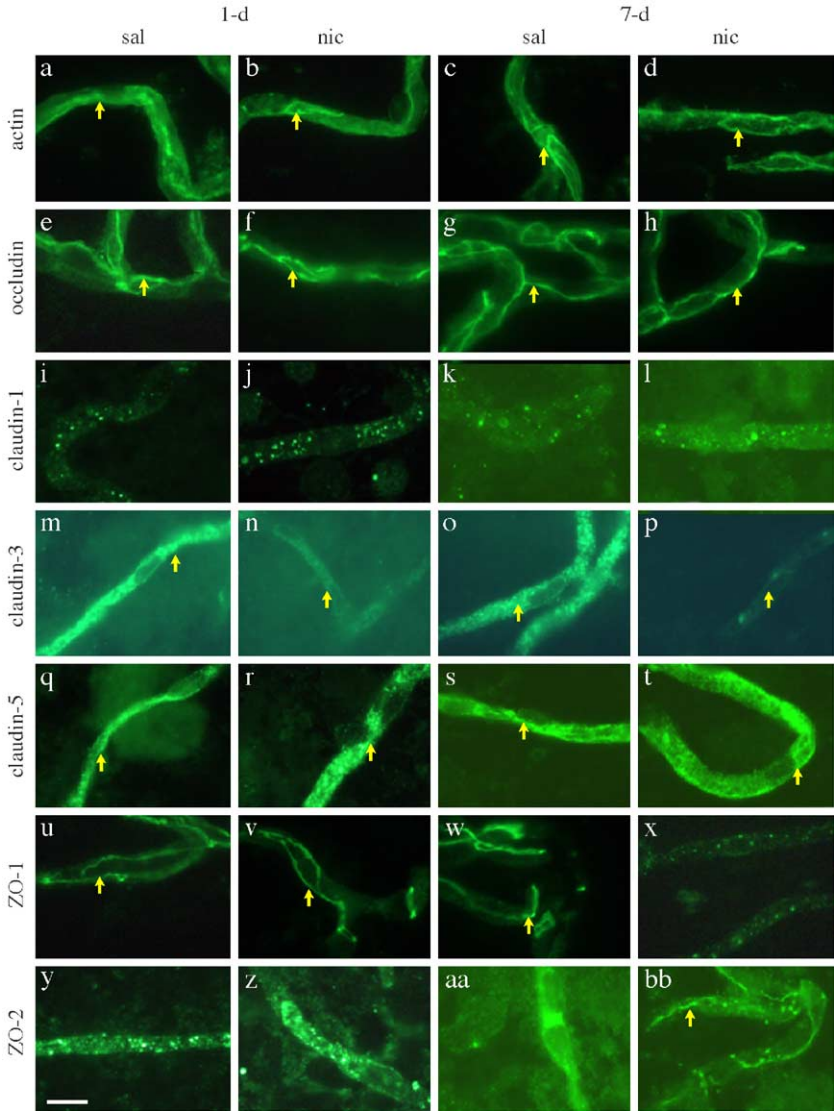

Fig. 3. Representative micrographs of BBB TJ proteins in brain microvessels. All proteins were visualized with mouse or rabbit primary antibody and Alexaflour™-488-conjugated secondary antibody. Secondary antibodies alone did not stain microvessels (data not shown). Each row, left to right: 1-day saline, 1-day nicotine, 7-day saline, 7-day nicotine. a–d: actin, e–h: occludin, i–l: claudin-1, m–p: claudin-3, q–t: claudin-5, u–x: ZO-1, y–bb: ZO-2. Arrows indicate areas of marginal distribution. All images are 100×. Scale bar=1 μm.

sacrifice. Nicotine eluted at a retention time of 4 min, cotinine at 5.5 min, and 2-phenylimidizole at 10 min. Nicotine and cotinine were not detected in naïve animals or in saline-treated controls. In the 1-day nicotine group, nicotine and cotinine plasma levels were 45.0±20.3 and 269.2±74.6 ng·ml^{-1} (n=3), respectively, and in the 7-day nicotine group, nicotine and cotinine levels were 71.7±37.3 and 261.6±35.5 ng·ml^{-1} (n=4), respectively. There was no statistically significant change in plasma nicotine or cotinine concentrations between 1 and 7 days.

3.2. Changes in BBB permeability

The effect of nicotine on BBB permeability was determined using in situ brain perfusion with [^{14}C]-sucrose (Fig. 1), a tracer that does not normally cross the BBB. Whole-brain visualization immediately following perfusion showed no appreciable leakage of Evans blue albumin into the parenchyma. Both 1- and 7-day nicotine treatments significantly increased the unidirectional transfer coefficients for sucrose from blood to brain (K_{in}) without a significant change in initial volume of distribution (V_D) relative to their time-matched controls (Table 1), indicating increased BBB permeability to sucrose. One-day nicotine treatment led to a 3.3-fold increase in K_{in}, from 0.6±0.2 to 2.0±0.3 μl·g^{-1}·min^{-1}. Seven-day nicotine treatment led to a four-fold increase in K_{in}, from 0.3±0.1 to 1.2±0.3 μl·g^{-1}·min^{-1}. Estimated V_D ranged from 1.0 to 7.0 μl·g^{-1}, which are comparable to previously published measurements [51]. No difference in K_{in} was observed between the 1- and 7-day saline-treated groups; however, a significant (p<0.05) decrease in K_{in} was detected in the 7-day nicotine treated group as compared to the 1-day nicotine treated group (Table 1).

3.3. Cerebral microvascular TJ protein expression

To determine if increased brain distribution of sucrose was due to an alteration of cerebral microvascular TJ, the expression of TJ-associated proteins occludin, claudin-1, -3, and -5, and ZO-1 and -2, and cytoskeletal actin in cerebral microvessels was assessed by semiquantitative Western blot analyses (Fig. 2). All antibodies recognized bands at or near the expected molecular weights of the target proteins in extracts from cerebral microvessels, with the exception of claudin-1 (Fig. 2B and D). Though trends towards decreased expression of claudin-3 following 1-day nicotine treatment (Fig. 2A) and ZO-1 following 7-day treatment (Fig. 2C) and increased actin expression following 7-day nicotine treatment (Fig. 2C) were noted, none of these changes were statistically significant in this analysis. No other changes in the expression of the proteins examined were observed.

3.4. Cerebral microvascular TJ protein distribution

To further investigate the possibility that alterations in BBB TJ were associated with the observed increase in BBB permeability, isolated cerebral microvessels were stained for the same proteins as above and visualized by immunofluorescence microscopy. In vessels from control animals, actin, occludin, claudin-3, claudin-5, and ZO-1 showed a predominant pattern of continuous staining along the margins of cell–cell contact (Fig. 3). ZO-2 showed strong immunoreactivity in cerebral microvessels, but with a much more diffuse pattern of staining (Fig. 3). Vessels stained for claudin-1 showed only very weak and diffuse immunoreactivity (Fig. 3). Alexfluor™ 488-conjugated anti-rabbit or anti-mouse IgG did not stain cerebral microvessels in the absence of a primary antibody (data not shown).

Changes in mean pixel intensity for each protein following nicotine treatment are summarized in Table 2. Vessels from animals treated with nicotine for 1 day showed a significant increase in staining for claudin-5, and a significant decrease in staining for claudin-3. A slight but statistically significant increase was also noted in actin staining in this group. Vessels from animals treated with nicotine for 7 days also showed a significant decrease in staining for claudin-3, but did not show any changes in actin or claudin-5. However, vessels from this group were also characterized by decreased mean pixel intensity of ZO-1 and increased mean pixel intensity of claudin-1 and ZO-2.

Qualitative examination of brain microvessels yielded the following observations. (1) In both 1- and 7-day nicotine-treated animals, the intensity of claudin-3 staining is greatly diminished throughout each vessel (Fig. 3n and p). (2) Vessels from 7-day nicotine-treated animals tend to have more continuous staining for ZO-2 than vessels from time-matched control animals (Fig. 3bb). (3) In vessels from 7-day nicotine-treated animals, the change in mean pixel intensity reflects an alteration in the cellular distribution of ZO-1. Specifically, there is a greater prevalence of a more

Table 2
Semiquantitative analysis of cerebral microvascular TJ proteins

	1-day		7-day	
	Saline	Nicotine	Saline	Nicotine
Actin	100.0±4.6	111.7±3.3*	100.0±3.6	98.3±4.2
Occludin	100.0±5.3	100.8±6.2	100.0±2.5	95.5±3.0
Claudin-1	100.0±6.4	111.7±5.1	100.0±6.0	131.7±8.1**
Claudin-3	100.0±3.5	35.9±3.7***	100.0±6.1	84.1±5.1*
Claudin-5	100.0±4.6	154.7±7.8***	100.0±2.6	104.6±3.0
ZO-1	100.0±6.6	110.2±4.7	100.0±5.7	79.4±5.5*
ZO-2	100.0±10.2	75.9±7.3	100.0±6.7	149.9±5.5***

Cerebral microvessels isolated from animals treated for 1 or 7 days with saline or nicotine were stained for tight junction-associated proteins. Images were captured and analyzed with Metamorph™. Mean pixel intensity was measured at randomly selected points along the margins of cell–cell contact (when visible) or at randomly selected points along each vessel in the absence of clear marginal distribution. Data are average corrected mean pixel intensity expressed as percentage of time-matched controls ±S.E.M. n=10–33 vessels for each group.

* p<0.05.

** p<0.005.

*** p<0.0005 vs. time-matched control.

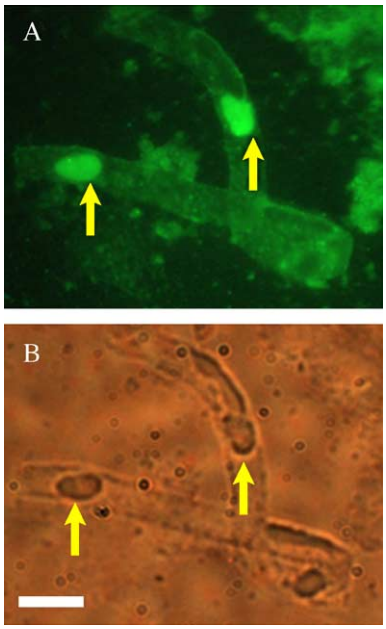

Fig. 4. Nuclear staining of ZO-1. A subset (~15%) of cerebral microvessels stained for ZO-1 in the 7-day nicotine group displayed large globular staining in the nuclear/perinuclear region of the endothelial cells, indicated by arrows. This was not observed in any other treatment group or naïve animals. (A) Fluorescent image, (B) phase contrast image of the same vessel. Images are 100×. Scale bar=1 μm.

diffuse, "punctuate" staining for ZO-1 and a loss of the clear marginal distribution observed in control animals (Fig. 3x). (4) In a subset of vessels harvested from 7-day nicotine-treated animals, there is intense globular staining for ZO-1 in what appears to be the nuclear/perinuclear region of cerebral microvascular endothelial cells, as confirmed by phase contrast visualization (Fig. 4). This was not observed in any vessels from any other group or naïve animals.

4. Discussion

4.1. Nicotine increases BBB permeability

In the current study, smoking was modeled by continuous subcutaneous administration of nicotine via an osmotic pump at 4.5 $mg \cdot kg^{-1} \cdot day^{-1}$. HPLC analysis confirmed that this regimen sustains nicotine and cotinine plasma levels comparable to those observed in chronic heavy smokers [39,61]. This is a useful criterion for evaluating the relevance of a nicotine treatment in light of the observation that habitual smokers regulate their smoking behavior to sustain a certain level of nicotine in their blood [30]. Moreover, rats trained to self-administer nicotine sustain plasma nicotine and cotinine levels in this range [50].

Though cigarette smoke contains many chemicals other than nicotine, nicotine administration imitates many of the vascular effects of smoking [28,47]. Furthermore, nicotine increases the volume of tissue damage in focal brain ischemia, depletes stores of tissue plasminogen activator (tPA) [61], increases levels of the endogenous inhibitor of tPA in the brain [67], and attenuates BBB Na,K,2Cl-cotransporter function under ischemic conditions [2]. Thus, nicotine is sufficient for producing a compromised state wherein the brain is potentially more vulnerable to cerebrovascular disease.

In this study, we investigated the effects of nicotine on BBB permeability using a modification of the Takasato in situ perfusion model [55]. This dual perfusion model has been well-characterized, and has been used to investigate drug delivery to the brain [40,56] and the effect of various pathologies [24,26,54] on the permeability of the BBB. Sucrose was chosen as a permeability marker because it has limited distribution to the brain parenchyma in naïve rats. Multiple-time uptake analysis (Fig. 1) was utilized allowing for analysis of the rate of sucrose uptake (K_{in}) and initial volume of distribution (V_D). In this study, the measured control values of K_{in} for sucrose were 0.6 ± 0.2 and 0.3 ± 0.1 $\mu l \cdot g^{-1} \cdot min^{-1}$ (1- and 7-day groups, respectively), similar to previously measured values [12]. One- and seven-day treatment with nicotine significantly increased the K_{in} for sucrose to 2.0 ± 0.3 and 1.2 ± 0.3 $\mu l \cdot g^{-1} \cdot min^{-1}$, respectively. Furthermore, nicotine did not significantly alter V_D in either group (Table 1). Thus, the increased uptake of sucrose into the brain following nicotine treatment likely reflects increased permeability of the BBB to sucrose rather than a change in V_D caused by nicotine.

Whereas Schilling et al. [49] only observed an increase in BBB permeability at toxic doses of nicotine, we have shown an increase in BBB permeability to sucrose (Fig. 1; Table 1) with nicotine plasma levels comparable to those seen in heavy smokers [39]. Sucrose, a smaller permeability marker, likely serves as a more sensitive indicator of TJ integrity at the BBB than the 70-kDa dextran used in the previous study [31]. Additionally, the route of administration in this study allows nicotine to be circulated rather than topically applied to the abluminal side of vessels in the brain. Finally, the previous study was limited to an acute effect of nicotine, while the current study evaluated the effects of constant nicotine infusion for up to a week. Thus, the current study is actually addressing a more chronic effect of nicotine on the BBB.

4.2. Nicotine alters BBB tight junctions

We hypothesized that nicotine-induced increases in BBB permeability to sucrose are due to an opening of the BBB mediated by alterations in the TJ. A number of conditions are known to increase the permeability of the BBB, including hypoxia and stroke, diabetes, multiple sclerosis, HIV, brain tumors, and peripheral inflammation; changes in the expression and/or organization of TJ proteins have been associated with increased permeability in all of these disease states [4,6,15,24,41,43]. Western blot analyses of the BBB TJ-associated proteins actin, occludin, claudin-1, -3, and -5, and ZO-1 and ZO-2 did not show a statistically significant change in the expression of any of these proteins in

microvessels from treated animals. These data suggest that the changes in BBB permeability may be due to changes in the organization of TJ proteins rather than changes in their expression.

An immunofluorescence staining protocol previously used on cultured brain microvessel endothelial cells (BMEC) [37] was adapted to probe for changes in TJ protein distribution in isolated microvessels. Representative photomicrographs of vessels stained for each of the proteins studied are shown in Fig. 3, in which the continuous marginal cellular distributions of occludin, claudin-3, claudin-5, and ZO-1 are apparent. Strong but discontinuous staining is observed for ZO-2, and weak diffuse staining is noted for claudin-1. These observations are in agreement with previous studies on brain microvessels [34]. Actin appears to be distributed at the margins and in the cytosol, as observed in BMEC cultures [37].

A semiquantitative technique was used to evaluate the continuity and/or strength of staining in cerebral microvessels. This approach has been used to demonstrate discontinuity of ZO-1 immunoreactivity in cerebral microvessels following treatment with monocyte chemoattractant protein-1 [52]. Among the TJ proteins that showed a consistent pattern of staining at the endothelial cell margins in control animals (ZO-1, occludin, claudin-3, and claudin-5), only ZO-1 showed a marked change in continuity of staining following nicotine treatment, and only in the 7-day treatment group (Fig. 3x). This was reflected in a significant decrease in mean pixel intensity for ZO-1 in this group (Table 2). Furthermore, a subset of vessels (~15%) from the 7-day nicotine-treated group stained strongly for ZO-1 at what appears to be the nucleus of cerebral microvessel endothelial cells (Fig. 4).

ZO-1 is regarded as a major regulatory component of the TJ. It is a member of the membrane-associated guanylate kinase (MAGUK) family of signaling proteins, and has multiple binding sites for protein–protein interactions [17]. ZO-1 links the transmembrane TJ protein occludin with the actin cytoskeleton [11]. Redistribution of ZO-1 away from the TJ has been observed in response to bacterial toxins [7], drugs [35], growth factors [23], cytokines [3], and hypoxia [14,15] and correlated with increased permeability and/or decreased electrical resistance.

An unexpected result was the apparent localization of ZO-1 at the endothelial nuclei of brain microvessels from the 7-day nicotine group. Though only a small proportion (15%) of the vessels observed showed ZO-1 at the nucleus, this is nonetheless important given that no vessels in any of the other treatment groups were observed to do so. Nuclear localization of ZO-1 has been observed in vitro, in subconfluent cells and near sites of wounding in confluent cultures [18], as well as following long-term calcium depletion [45]. In both studies, localization of ZO-1 to the nucleus was strongly associated with limited contact between cells and was reversible upon establishment of cell–cell contact. It is therefore unclear whether nuclear localization of ZO-1 in this case is associated with abnormal proliferation of cerebral microvessels in response to nicotine [20] or reflects a loss of cell–cell contacts mediated via another constituent of the TJ.

Another surprising observation was the apparent translocation of ZO-2 to the cellular margins in the 7-day nicotine-treated group (Fig. 3bb). ZO-2 has been found at the TJ of epithelial cells under normal conditions, and localizes to the nucleus under certain conditions of stress and growth [29,57]. The normal localization of ZO-2 in cerebral microvessels has not been characterized previously. In vessels from control animals in this study, ZO-2 displayed diffuse immunoreactivity throughout the endothelial cells, indicating that it may not play an important role in BBB TJ under normal circumstances. Interestingly, Huber et al. [27] noted an increased association between ZO-1 and ZO-2 under conditions of increased permeability. However, ZO-1 immunoreactivity at the cellular margins is decreased by nicotine in this study. It is therefore difficult to discern what increased immunoreactivity of ZO-2 at the cell margins signifies in this case, though it may reflect increased association with one of the more stable components of the TJ such as occludin or claudin-5 enabled by the dissociation of ZO-1 from the junctional complex.

The intensity of claudin-3 staining was diminished in both 1- and 7-day nicotine-treated groups (Table 2), although this does not appear to involve the same redistribution away from the cellular margins observed with ZO-1 (Fig. 3n and p). Why this apparent decrease in the amount of claudin-3 expressed in cerebral microvessels would not be reflected in Western blot analysis is unclear; however, it is important to note that the molecular environment in which the antibody binds claudin-3 is very different in the two experiments (i.e., fixed, permeabalized tissue vs. protein extracts in SDS), and this may contribute to the difference in results. Claudin-3 has only recently been identified as a key component of BBB TJ, and the selective loss of claudin-3 is associated with increased permeability [64]. We observed diminished immunoreactivity of claudin-3 while claudin-5 remained relatively constant (Fig. 3m–t, claudin-5 intensity was increased in 1-day treated animals relative to control). Furthermore, using a newer antibody that does not cross-react with claudin-3, claudin-1 immunoreactivity was weak in cerebral microvessels and not associated with the margins of cell–cell contact nor observed on Western blots, as previously reported [63]. Thus, the current study is consistent with the hypothesis proposed by Wolburg et al. [64] that claudin-3 is a major determinant of in vivo BBB permeability independent of claudin-5 and occludin.

4.3. Conclusion

This is the first study to report a significant increase in the basal permeability of the BBB induced by nicotine at a pharmacologically relevant dose in vivo. This is also the

first report of nuclear localization of ZO-1 at the cerebral microvascular endothelium, as well as the first reported observation of this phenomenon in a native tissue. Whether translocation of ZO-1 is indicative of abnormal proliferation of cerebral microvessels or reflects a loss of cell–cell contacts associated with diminished immunoreactivity for claudin-3 is not certain, as either situation could be associated with increased BBB permeability. These cellular responses to nicotine suggest a role for nicotinic acetylcholine receptors, possibly expressed on the vascular endothelium itself [1,36,38], in the regulation of BBB TJ and permeability. Further attention to the complex interactions of TJ proteins at the BBB is warranted to discern the mechanisms by which nicotine compromises the BBB, and how this phenomenon may impact the development and progression of neurological diseases in which diminished BBB function is critical.

Acknowledgements

This work was supported by NIH grants NS 39592, DA 11271, and Arizona Disease Control Research Commission contract 5011 to T.P.D, NS 046526 to T.J.A., DK 065003 to R.D.E., NRSA DA 06037 to J.D.H., and NRSA NS 43052 to R.C.B.

References

[1] T.J. Abbruscato, S.P. Lopez, K.S. Mark, B.T. Hawkins, T.P. Davis, Nicotine and cotinine modulate cerebral microvascular permeability and protein expression of ZO-1 through nicotinic acetylcholine receptors expressed on brain endothelial cells, J. Pharm. Sci. 91 (2002) 2525–2538.

[2] T.J. Abbruscato, S.P. Lopez, K. Roder, J.R. Paulson, Regulation of blood–brain barrier Na,K,2Cl-cotransporter through phosphorylation during in vitro stroke conditions and nicotine exposure, J. Pharmacol. Exp. Ther. 310 (2004) 459–468.

[3] M.S. Blum, E. Toninelli, J.M. Anderson, M.S. Balda, J. Zhou, L. O'Donnell, R. Pardi, J.R. Bender, Cytoskeletal rearrangement mediates human microvascular endothelial tight junction modulation by cytokines, Am. J. Physiol. 273 (1997) H286–H294.

[4] L.A. Boven, J. Middel, J. Verhoef, C.J. De Groot, H.S. Nottet, Monocyte infiltration is highly associated with loss of the tight junction protein zonula occludens in HIV-1-associated dementia, Neuropathol. Appl. Neurobiol. 26 (2000) 356–3560.

[5] CDC, State-specific prevalence of current cigarette smoking among adults—United States, 2002, Morb. Mortal. Wkly. Rep. 52 (2004) 1277–1280.

[6] J.M. Chehade, M.J. Haas, A.D. Mooradian, Diabetes-related changes in rat cerebral occludin and zonula occludens-1 (ZO-1) expression, Neurochem. Res. 27 (2002) 249–252.

[7] M.L. Chen, C. Pothoulakis, J.T. LaMont, Protein kinase C signaling regulates ZO-1 translocation and increased paracellular flux of T84 colonocytes exposed to Clostridium difficile toxin A, J. Biol. Chem. 277 (2002) 4247–4254.

[8] R. Dawson, S.M. Messina, C. Stokes, S. Salyani, N. Alcalay, N.C. de Fiebre, C.M. de Fiebre, Solid-phase extraction and HPLC assay of nicotine and cotinine in plasma and brain, Toxicol. Mech. Methods 12 (2002) 45–58.

[9] R. Duelli, R. Staudt, F. Grunwald, W. Kuschinsky, Increase of glucose transporter densities (Glut1 and Glut3) during chronic administration of nicotine in rat brain, Brain Res. 782 (1998) 36–42.

[10] R. Duelli, R. Staudt, M.H. Maurer, W. Kuschinsky, Local transport kinetics of glucose during acute and chronic nicotine infusion in rat brains, J. Neural Transm. 105 (1998) 1017–1028.

[11] A.S. Fanning, B.J. Jameson, L.A. Jesaitis, J.M. Anderson, The tight junction protein ZO-1 establishes a link between the transmembrane protein occludin and the actin cytoskeleton, J. Biol. Chem. 273 (1998) 29745–29753.

[12] J. Fenstermacher, S.I. Rapoport, The blood–brain barrier, in: E.M. Renkin, C.C. Michel (Eds.), Handbook of Physiology: The Microcirculation, Am. Physiol. Soc., Bethesda, MD, 1984, pp. 969–1000.

[13] J. Fenstermacher, P. Gross, N. Sposito, V. Acuff, S. Pettersen, K. Gruber, Structural and functional variations in capillary systems within the brain, Ann. N.Y. Acad. Sci. 529 (1988) 21–30.

[14] S. Fischer, M. Clauss, M. Wiesnet, D. Renz, W. Schaper, G.F. Karliczek, Hypoxia induces permeability in brain microvessel endothelial cells via VEGF and NO, Am. J. Physiol. 276 (1999) C812–C820.

[15] S. Fischer, M. Wobben, H.H. Marti, D. Renz, W. Schaper, Hypoxia-induced hyperpermeability in brain microvessel endothelial cells involves VEGF-mediated changes in the expression of zonula occludens-1, Microvasc. Res. 63 (2002) 70–80.

[16] S.A. Glantz, Primer of Biostatistics, 5th ed., McGraw Hill, New York, 2002.

[17] L. Gonzalez-Mariscal, A. Betanzos, A. Avila-Flores, MAGUK proteins: structure and role in the tight junction, Semin. Cell Dev. Biol. 11 (2000) 315–324.

[18] C.J. Gottardi, M. Arpin, A.S. Fanning, D. Louvard, The junction-associated protein, zonula occludens-1, localizes to the nucleus before the maturation and during the remodeling of cell–cell contacts, Proc. Natl. Acad. Sci. U. S. A. 93 (1996) 10779–10784.

[19] B.T. Hawkins, R.C. Brown, T.P. Davis, Smoking and ischemic stroke: a role for nicotine? Trends Pharmacol. Sci. 23 (2002) 78–82.

[20] C. Heeschen, J.J. Jang, M. Weis, A. Pathak, S. Kaji, R.S. Hu, P.S. Tsao, F.L. Johnson, J.P. Cooke, Nicotine stimulates angiogenesis and promotes tumor growth and atherosclerosis, Nat. Med. 7 (2001) 833–839.

[21] C. Heeschen, M. Weis, A. Aicher, S. Dimmeler, J.P. Cooke, A novel angiogenic pathway mediated by non-neuronal nicotinic acetylcholine receptors, J. Clin. Invest. 110 (2002) 527–536.

[22] D. Hoffmann, I. Hoffmann, The changing cigarette, 1950–1995, J. Toxicol. Environ. Health 50 (1997) 307–364.

[23] F. Hollande, E.M. Blanc, J.P. Bali, R.H. Whitehead, A. Pelegrin, G.S. Baldwin, A. Choquet, HGF regulates tight junctions in new non-tumorigenic gastric epithelial cell line, Am. J. Physiol.: Gastrointest. Liver Physiol. 280 (2001) G910–G921.

[24] S. Hom, R.D. Egleton, J.D. Huber, T.P. Davis, Effect of reduced flow on blood–brain barrier transport systems, Brain Res. 890 (2001) 38–48.

[25] J.D. Huber, R.D. Egleton, T.P. Davis, Molecular physiology and pathophysiology of tight junctions in the blood–brain barrier, Trends Neurosci. 24 (2001) 719–725.

[26] J.D. Huber, K.A. Witt, S. Hom, R.D. Egleton, K.S. Mark, T.P. Davis, Inflammatory pain alters blood–brain barrier permeability and tight junctional protein expression, Am. J. Physiol., Heart Circ. Physiol. 280 (2001) H1241–H1248.

[27] J.D. Huber, V.S. Hau, L. Borg, C.R. Campos, R.D. Egleton, T.P. Davis, Blood–brain barrier tight junctions are altered during a 72-h exposure to lambda-carrageenan-induced inflammatory pain, Am. J. Physiol., Heart Circ. Physiol. 283 (2002) H1531–H1537.

[28] M. Iida, H. Iida, S. Dohi, M. Takenaka, H. Fujiwara, Mechanisms underlying cerebrovascular effects of cigarette smoking in rats in vivo, Stroke 29 (1998) 1656–1665.

[29] S. Islas, J. Vega, L. Ponce, L. Gonzalez-Mariscal, Nuclear localization of the tight junction protein ZO-2 in epithelial cells, Exp. Cell Res. 274 (2002) 138–148.

[30] M.E. Jarvik, D.C. Madsen, R.E. Olmstead, P.N. Iwamoto-Schaap, J.L. Elins, N.L. Benowitz, Nicotine blood levels and subjective craving for cigarettes, Pharmacol. Biochem. Behav. 66 (2000) 553–558.
[31] M. Juhler, D.I. Barry, H. Offner, G. Konat, L. Klinken, O.B. Paulson, Blood–brain and blood–spinal cord barrier permeability during the course of experimental allergic encephalomyelitis in the rat, Brain Res. 302 (1984) 347–355.
[32] R.F. Keep, L.J. Ulanski II, J. Xiang, S.R. Ennis, A. Lorris Betz, Blood–brain barrier mechanisms involved in brain calcium and potassium homeostasis, Brain Res. 815 (1999) 200–205.
[33] U. Kniesel, H. Wolburg, Tight junctions of the blood–brain barrier, Cell. Mol. Neurobiol. 20 (2000) 57–76.
[34] A. Lippoldt, U. Kniesel, S. Liebner, H. Kalbacher, T. Kirsch, H. Wolburg, H. Haller, Structural alterations of tight junctions are associated with loss of polarity in stroke-prone spontaneously hypertensive rat blood–brain barrier endothelial cells, Brain Res. 885 (2000) 251–261.
[35] D.Z. Liu, E.L. LeCluyse, D.R. Thakker, Dodecylphosphocholine-mediated enhancement of paracellular permeability and cytotoxicity in Caco-2 cell monolayers, J. Pharm. Sci. 88 (1999) 1161–1168.
[36] K.D. Macklin, A.D. Maus, E.F. Pereira, E.X. Albuquerque, B.M. Conti-Fine, Human vascular endothelial cells express functional nicotinic acetylcholine receptors, J. Pharmacol. Exp. Ther. 287 (1998) 435–439.
[37] K.S. Mark, T.P. Davis, Cerebral microvascular changes in permeability and tight junctions induced by hypoxia–reoxygenation, Am. J. Physiol., Heart Circ. Physiol. 282 (2002) H1485–H1494.
[38] F. Moccia, C. Frost, R. Berra-Romani, F. Tanzi, D.J. Adams, Expression and function of neuronal nicotinic ACh receptors in rat microvascular endothelial cells, Am. J. Physiol., Heart Circ. Physiol. 286 (2004) H486–H491.
[39] L.C. Murrin, J.R. Ferrer, W.Y. Zeng, N.J. Haley, Nicotine administration to rats: methodological considerations, Life Sci. 40 (1987) 1699–1708.
[40] W. Pan, A.J. Kastin, J.M. Brennan, Saturable entry of leukemia inhibitory factor from blood to the central nervous system, J. Neuroimmunol. 106 (2000) 172–180.
[41] M.C. Papadopoulos, S. Saadoun, D.C. Davies, B.A. Bell, Emerging molecular mechanisms of brain tumour oedema, Br. J. Neurosurg. 15 (2001) 101–108.
[42] K.A. Perkins, J.E. Sexton, W.A. Reynolds, J.E. Grobe, C. Fonte, R.L. Stiller, Comparison of acute subjective and heart rate effects of nicotine intake via tobacco smoking versus nasal spray, Pharmacol. Biochem. Behav. 47 (1994) 295–299.
[43] J. Plumb, S. McQuaid, M. Mirakhur, J. Kirk, Abnormal endothelial tight junctions in active lesions and normal-appearing white matter in multiple sclerosis, Brain Pathol. 12 (2002) 154–169.
[44] T.S. Reese, M.J. Karnovsky, Fine structural localization of a blood–brain barrier to exogenous peroxidase, J. Cell Biol. 34 (1967) 207–217.
[45] F.K. Riesen, B. Rothen-Rutishauser, H. Wunderli-Allenspach, A ZO1-GFP fusion protein to study the dynamics of tight junctions in living cells, Histochem. Cell Biol. 117 (2002) 307–315.
[46] I.A. Romero, K. Radewicz, E. Jubin, C.C. Michel, J. Greenwood, P.O. Couraud, P. Adamson, Changes in cytoskeletal and tight junctional proteins correlate with decreased permeability induced by dexamethasone in cultured rat brain endothelial cells, Neurosci. Lett. 344 (2003) 112–116.
[47] M. Sabha, J.E. Tanus-Santos, J.C. Toledo, M. Cittadino, J.C. Rocha, H. Moreno Jr., Transdermal nicotine mimics the smoking-induced endothelial dysfunction, Clin. Pharmacol. Ther. 68 (2000) 167–174.
[48] J.M. Scherrmann, Drug delivery to brain via the blood–brain barrier, Vasc. Pharmacol. 38 (2002) 349–354.
[49] L. Schilling, A. Bultmann, M. Wahl, Lack of effect of topically applied nicotine on pial arteriole diameter and blood–brain barrier integrity in the cat, Clin. Investig. 70 (1992) 210–217.
[50] M. Shoaib, I.P. Stolerman, Plasma nicotine and cotinine levels following intravenous nicotine self-administration in rats, Psychopharmacology (Berl.) 143 (1999) 318–321.
[51] Q.R. Smith, Y.Z. Ziylan, P.J. Robinson, S.I. Rapoport, Kinetics and distribution volumes for tracers of different sizes in the brain plasma space, Brain Res. 462 (1988) 1–9.
[52] L. Song, J.S. Pachter, Monocyte chemoattractant protein-1 alters expression of tight junction-associated proteins in brain microvascular endothelial cells, Microvasc. Res. 67 (2004) 78–89.
[53] W. Stummer, R.F. Keep, A.L. Betz, Rubidium entry into brain and cerebrospinal fluid during acute and chronic alterations in plasma potassium, Am. J. Physiol. 266 (1994) H2239–H2246.
[54] H. Suzuki, T. Nagashima, K. Fujita, N. Tamaki, K. Sugioka, T. Yamadori, M. Yamaguchi, Cerebral ischemia alters glucose transporter kinetics across rat brain microvascular endothelium. Quantitative analysis by an in situ brain perfusion method, J. Auton. Nerv. Syst. 49 (1994) S173–S176 (Suppl).
[55] Y. Takasato, S.I. Rapoport, Q.R. Smith, An in situ brain perfusion technique to study cerebrovascular transport in the rat, Am. J. Physiol. 247 (1984) H484–H493.
[56] S.A. Thomas, A. Bye, M.B. Segal, Transport characteristics of the anti-human immunodeficiency virus nucleoside analog, abacavir, into brain and cerebrospinal fluid, J. Pharmacol. Exp. Ther. 298 (2001) 947–953.
[57] A. Traweger, R. Fuchs, I.A. Krizbai, T.M. Weiger, H.C. Bauer, H. Bauer, The tight junction protein ZO-2 localizes to the nucleus and interacts with the hnRNP protein SAF-B, J. Biol. Chem. 27 (2002) 27.
[58] A.C. Villablanca, Nicotine stimulates DNA synthesis and proliferation in vascular endothelial cells in vitro, J. Appl. Physiol. 84 (1998) 2089–2098.
[59] A.W. Vorbrodt, D.H. Dobrogowska, Molecular anatomy of intercellular junctions in brain endothelial and epithelial barriers: electron microscopist's view, Brain Res. Brain Res. Rev. 42 (2003) 221–242.
[60] L. Wang, J.G. McComb, M.H. Weiss, A.A. McDonough, B.V. Zlokovic, Nicotine downregulates alpha 2 isoform of Na,K-ATPase at the blood–brain barrier and brain in rats, Biochem. Biophys. Res. Commun. 199 (1994) 1422–1427.
[61] L. Wang, M. Kittaka, N. Sun, S.S. Schreiber, B.V. Zlokovic, Chronic nicotine treatment enhances focal ischemic brain injury and depletes free pool of brain microvascular tissue plasminogen activator in rats, J. Cereb. Blood Flow Metab. 17 (1997) 136–146.
[62] W. Wang, W.L. Dentler, R.T. Borchardt, VEGF increases BMEC monolayer permeability by affecting occludin expression and tight junction assembly, Am. J. Physiol., Heart Circ. Physiol. 280 (2001) H434–H440.
[63] K.A. Witt, K.S. Mark, S. Hom, T.P. Davis, Effects of hypoxia–reoxygenation on rat blood–brain barrier permeability and tight junctional protein expression, Am. J. Physiol., Heart Circ. Physiol. 285 (2003) H2820–H2831.
[64] H. Wolburg, K. Wolburg-Buchholz, J. Kraus, G. Rascher-Eggstein, S. Liebner, S. Hamm, F. Duffner, E.H. Grote, W. Risau, B. Engelhardt, Localization of claudin-3 in tight junctions of the blood–brain barrier is selectively lost during experimental autoimmune encephalomyelitis and human glioblastoma multiforme, Acta Neuropathol. 105 (2003) 586–592.
[65] S. Zhang, I. Day, S. Ye, Nicotine induced changes in gene expression by human coronary artery endothelial cells, Atherosclerosis 154 (2001) 277–283.
[66] S. Zhang, I.N. Day, S. Ye, Microarray analysis of nicotine-induced changes in gene expression in endothelial cells, Physiol. Genomics 5 (2001) 187–192.
[67] R. Zidovetzki, P. Chen, M. Fisher, F.M. Hofman, F.M. Faraci, Nicotine increases plasminogen activator inhibitor-1 production by human brain endothelial cells via protein kinase C-associated pathway, Stroke 30 (1999) 651–655.